European Journal of Immunology

Renal medullary osmolytes NaCl and urea differentially modulate human tubular cell cytokine expression and monocyte recruitment

Jessica Schmitz[1]*, Nicolas Brauns[2]*, Anne M. Hüsing[2], Martina Flechsig[2],

Thorsten Glomb[3], Jan Hinrich Bräsen[1], Hermann Haller[2], and Sibylle von Vietinghoff[2,4]

[1]Nephropathology Unit, Institute for Pathology,
[2]Department of Internal Medicine, Division of Nephrology and Hypertension,
[3]Core Facility Transcriptomics, Hannover Medical School, Hannover, and
[4]Nephrology Section, First Medical Clinic, University Clinic and Rheinische Friedrich-Wilhelms Universität Bonn, Bonn, Germany
*These authors contributed equally.

Keywords: monocyte, chemokine, renal tubular epithelium, NaCl, urea

Address correspondence to:
Sibylle von Vietinghoff
Nephrology Section, First Medical Clinic
University Clinic Bonn
Venusberg Campus 1
D-53127 Bonn
Phone: +49-(0)228-287-15767
FAX: +49-(0)228-287-14956
Sibylle.von_Vietinghoff@ukbonn.de

Abstract

Renal immune cells serve as sentinels against ascending bacteria but also promote detrimental inflammation. The kidney medulla is characterized by extreme electrolyte concentrations. We here address how its main osmolytes, NaCl and urea, regulate tubular cell cytokine expression and monocyte chemotaxis.

In the healthy human kidney, more monocytes were detected in medulla than cortex. The monocyte gradient was attenuated in patients with medullary NaCl depletion by loop diuretic therapy and in the nephrotic syndrome. Renal tubular epithelial cell gene expression responded similarly to NaCl and tonicity control mannitol, but not urea. NaCl significantly upregulated chemotactic cytokines, most markedly *CCL26*, *CCL2* and *CSF1*. This induction was inhibited by ROS scavenger

Received: 15/11/2021; Revised: 06/05/2022; Accepted: 06/05/2022

This article has been accepted for publication and undergone full peer review but has not been through the copyediting, typesetting, pagination and proofreading process, which may lead to differences between this version and the Version of Record. Please cite this article as doi: 10.1002/eji.202149723.

n-acetylcysteine. In contrast urea, the main medullary osmolyte in catabolism, dampened tubular epithelial *CCL26* and *CSF1* expression. Renal medullary chemokine and monocyte marker expression decreased in catabolic mice. NaCl-, but not urea-stimulated tubular epithelium or CCL2 and CCL26 promoted human classical monocyte migration. CCL26 improved bactericidal function. In the human kidney medulla, monocyte densities correlated with tubular CCL26 protein abundance.

In summary, medullary-range NaCl, but not urea, promotes tubular cytokine expression and monocyte recruitment. This may contribute to the pyelonephritis vulnerability in catabolism but can possibly be harnessed against pathologic inflammation.

Introduction

In order to achieve up to 1200mOsm in the urine, the human kidney establishes a marked osmotic gradient [1]. It is adapted to volume status and rises with the need for water conservation. The main medullary osmotic agents are sodium chloride (NaCl) and urea. Urea replaces NaCl as main osmolyte in catabolism [2]. This includes the somewhat unexpected recent observation that a high salt diet induces a catabolic state that enhances medullary urea, rather than NaCl concentrations [2],[3]. Renal medullary NaCl is depleted by acute and chronic loop diuretic use [4]–[6] or in the nephrotic syndrome [7],[8].

The kidney medulla contains resident myeloid cells, namely monocytes and macrophages. Myeloid cells are central for the renal medullary immune response [9],[10]. Monocytes and macrophages recruit neutrophilic granulocytes, the body's main line of immediate antibacterial response, into the urinary tract [11],[12]. On the other hand, renal macrophage densities predict adverse outcome of inflammatory kidney conditions including autoimmune vasculitides and loss of transplant function [13].

Human gene expression and murine lineage tracking data suggest that renal myeloid cells are of embryonic and of monocytic origin [14]–[17]. Marker analysis and bioinformatic estimates propose preferential localization of $CD14^+$ monocytic cells to the medulla [11],[14]. Indeed, elevated NaCl concentrations enhance renal tubular epithelial cell secretion of the monocyte chemotactic cytokine CCL2 [11],[18]. How NaCl regulates other tubular cell cytokines and underlying mechanisms have

not been reported. Also, how the other main medullary osmolyte, urea, affects the tubular phenotype regarding chemokine expression has not been detailed.

We found that monocyte enrichment in the human kidney medulla varied with conditions that modulate local NaCl concentration. Therefore, we addressed mechanisms by which renal medullary-range NaCl and urea can affect monocyte migration. Medullary-range hypertonic NaCl, but not urea, dose- and time-dependently induced monocyte chemoattractant expression and recruitment by tubular epithelium. Our data delineate the human cytokine CCL26 as a novel cooperative monocyte chemoattractant that is induced by NaCl, but suppressed by medullary range urea.

Results

Monocyte enrichment in the human kidney medulla correlates with the concentration gradient

Renal innate immune cells centrally modulate antibacterial host response as well as detrimental inflammation. We sought to morphologically define monocyte and macrophage distribution in the human kidney. Their abundance was assessed in histologically normal human kidney tissue (figure 1A). We used digitally assisted pathology of whole slide scans as previously described and detailed in methods to quantify infiltrates [18],[19]. $CD14^+$ monocytes were significantly more abundant in medulla than cortex (figure 1A-C). This confirms measurements and bioinformatics estimates in other cohorts [11],[14]. The densities of $CD68^+$ macrophages did not differ significantly between the compartments (figure 1B,C). Very few neutrophils were found (suppl. figure 1).

We previously demonstrated induction of tubular monocyte chemotactic chemokine CCL2 expression by NaCl [18]. To determine whether renal monocyte distribution associates with the medullary salt gradient, we identified patient groups with clinical conditions known to alter the salt gradient that were sufficiently frequently biopsied and assessed monocyte densities in their kidney compartments.

First, loop diuretic therapy depletes the medullary salt gradient [4]–[6]. Its effect on monocyte distribution to cortex and medulla was studied in early surveillance biopsies of renal allografts.

Clinical characteristics are given in suppl. table 1. Immunosuppressant regimens were very similar. There was no significant difference in rejection frequency or other characteristics defined by the Banff classification. Absolute monocyte densities were similar and higher in medulla than cortex in both subgroups (figure 1D, suppl. figure 2). In addition, relative medullary $CD14^+$ monocyte accumulation was significantly more marked in grafts without diuretic therapy (figure 1E). This occurred despite the fact that loop diuretic recipients' grafts were more often cadaveric and had lower excretory function. The finding is consistent with a role of the NaCl gradient in their accumulation.

Second, the renal salt gradient is depleted in the nephrotic syndrome [7],[8]. We therefore studied renal monocyte and macrophage distribution in minimal change disease. Native kidney biopsies with an exclusive diagnosis of minimal change disease in patients without concomitant immunosuppression were assessed (figure 1F,G, clinical characteristics in suppl. table 2). Already in patients without diuretic therapy at the time of biopsy, absolute medullary $CD14^+$ monocyte density and relative accumulation compared to the cortex were significantly less than in healthy controls (Dunn's after Kruskal Wallis test, figure 1C,G). In the subgroup of minimal change disease patients who received a loop diuretic at the time of biopsy, the medullo-cortical monocyte gradient was no longer significant (figure 1G).

Taken together, medullary $CD14^+$ monocyte enrichment was observed in human kidneys. It was dampened and even abolished in conditions known for a reduced medullary salt gradient.

Equiosmolar NaCl and urea differentially regulate renal tubular epithelial gene expression

Induction of tubular chemotactic chemokine CCL2 expression by NaCl [18] lead to the hypothesis that the association of medullary monocyte accumulation with the concentration-gradient in vivo was functionally mediated by tubular cell chemokine production. To systematically investigate tubular cell response to increases in ambient NaCl and urea, we conducted gene expression studies.

HK2 human renal tubular epithelial cell gene expression was assessed after 24h culture with either additional 120mM NaCl or equiosmolar 240mM urea and compared to standard media and 240mM mannitol as a tonicity control. Genes regulated more than twofold in relation to normal media were compared for the three hyperosmolar conditions (figure 2A). There was a major overlap between

the hypertonic stimuli mannitol and NaCl, and markedly less with equiosmolar urea. This was also evident in principal component analyses (figure 2B,C). Similarly, heatmap analysis shows that a large proportion of the genes upregulated by NaCl was also upregulated by increased tonicity in the mannitol condition (figure 2D). The response to urea was more similar to the standard media control. It is of note that parallel regulation by NaCl and urea was significantly less common in the up- than in the downregulated fraction of genes (figure 2A). These data delineate a distinct tubular cell response to the main medullary osmolytes NaCl and urea.

NaCl, but not urea, induces tubular cell chemokine expression

To address tubular cell derived recruitment cues in response to NaCl and urea, chemokine, cytokine and interleukin expression was analyzed in detail. Among all detected factors, 14 were up- and 9 downregulated 1.5x or more by hypertonic NaCl (figure 3A). Modulation by NaCl and mannitol was largely parallel, similar to what was observed for all genes (figure 2). *CCL26*, *CCL2* and *CSF1* were most differentially expressed in hypertonicity compared to controls (figure 3B). This was maximal after 24h exposure (figure 3C). No such effect was observed if a lower amount of NaCl (+40mM) or equimolar urea concentrations were added (figure 3C). Mannitol of equal tonicity induced these chemokines to a similar extent as NaCl, consistent with a tonicity driven, substance independent process (figure 3D). Indeed, scavenging of ROS with a known role in mediation of tonicity-responses [20]–[22] using n-acetylcysteine (NAC) completely prevented NaCl induced *CCL26*, *CCL2* and *CSF1* mRNA expression (figure 3E). These results introduce CCL26 as a NaCl-regulated chemokine and define a ROS-dependent tonicity response as underlying mechanism.

The human kidney expresses CCL26 predominantly in the medulla

Indeed, CCL26 was expressed in the human kidney on protein and mRNA levels (figure 4A,B). To explore which of the NaCl-regulated mediators were present and similarly regulated in the human kidney, all chemotactic genes upregulated at least 1.5x by NaCl (figure 3A) were analyzed in healthy human medulla and compared to cortex (GSE3931)[23]. Among upregulated genes, *CCL26*, which was most enhanced by NaCl in tubular cells in vitro, also showed the strongest trend to increase in vivo (figure 4C). Among downregulated chemotactic factors, there was a similar

medullary trend for *IL32* (suppl. figure 3A). We next stained for CCL26 in normal human kidney sections. It was mostly expressed by proximal tubuli (figure 4D). Tubular CCL26 was significantly more abundant in medulla than cortex (figure 4E,F), introducing CCL26 as a novel human kidney medullary chemokine.

Suppression of tubular cytokine expression by urea

The role of urea for human tubular cytokine expression was addressed next. Our gene expression screen suggested downregulation of several chemoattractants by urea (figure 3A). The most regulated *CCL26*, *CCL2* and *CSF1* were studied further. Addition of 240mM urea suppressed the effect of NaCl on *CCL26* and *CSF1,* but not *CCL2* mRNA (figure 5A). To test whether this inhibition also applies to other CCL26 inducers, we employed IL-4 and IL-13 that promote *CCL26* expression in other celltypes [24]–[27]. *IL13* expression was detectable in the normal human kidney medulla (GSE3931, data not shown). Both IL-4 and IL-13 markedly enhanced *CCL26* expression in human renal tubular epithelium (figure 5B). There was a cooperative effect with elevated NaCl concentration (suppl. figure 4). In contrast, medullary range urea significantly inhibited cytokine-induced tubular epithelial *CCL26* (figure 5B). These data demonstrate suppressive function of urea on expression of distinct human tubular cell chemokines.

Suppression of renal medullary cytokine expression in catabolism in vivo

In vivo, urea accumulates in the renal medulla in catabolism, as investigated in detail in mice during a high salt diet [2]. As patients are rarely biopsied in this condition, we analyzed a renal gene expression dataset [21] of volume-depleted and severely catabolic mice after 72h of water restriction (figure 6A). Their food intake was 19% of controls. Gene expression in cortex and inner stripe of outer medulla was compared in catabolic mice and controls. Consistent with published functional data [2],[3], urea, but not sodium transporter expression increased in this state (suppl. figure 5). Overall, immune response pathways were prominently more expressed in normal than catabolic medulla (suppl. figure 6A), which is consistent with an enhancement by NaCl and dampening by urea. NaCl-mediated upregulation would also imply that these genes should be expressed at higher levels in normal medulla than normal cortex. Indeed, genes upregulated in both comparisons, i.e. normal

medulla versus normal cortex and normal medulla versus catabolic medulla, contained similar functional groups (suppl. figure 6B). A number of chemokines and receptors were detected (suppl. figure 6C). Visualization of all common upregulated pathways in this double comparison, i.e. in normal medulla compared to normal cortex and normal compared to catabolic medulla underlines a prominent position of immunoregulatory genes (suppl. figure 6D).

Monocytic gene expression was analyzed based on the histologic results in the human kidney (figure 1, [11]). Macrophage marker CD68, murine monocyte marker CD115 (*Csfr1*) and nonclassical monocyte/DC marker CX3CR1 were expressed to higher levels in the murine kidney medulla than cortex in resting conditions, while classical monocyte marker CCR2 was higher in the cortex (figure 6B,C). In catabolism, CD68 and CX3CR1 dropped significantly in the medulla. Also, expression the MHCII molecule H2Aa as M1 polarization marker dropped more than M2 marker CD206 in the medulla of catabolic mice (figure 6D), consistent with a regulation by NaCl and in parallel with our earlier results in the human kidney [18].

Soluble chemotactic factors produced by tubular epithelium were analyzed next (figure 6E). *CCL26* is a pseudogene in mice [28]. Renal medullary CSF1 mRNA expression was downregulated in catabolism, CCL2 and IL-1β mRNA were not significantly affected when compared to control medulla. With the human NaCl-regulated chemokine system in view (suppl. figure 3C), we investigated other human CCL26 receptors to explore for parallel responses in humans and mice that are observed for most types of inflammation [29] (figure 6F). Indeed, *Ccr5* and its ligand *Ccl3* were expressed significantly higher in resting medulla than cortex (figure 6G). This was abrogated in catabolism, consistent with a NaCl-dependent regulation.

To address whether this could be attributed to catabolism, a second independent dataset of more moderate catabolism was analyzed [30]. Here, four weeks caloric restriction decreased body weight to 76% and doubled serum urea (figure 6H). We analyzed regulation of chemokines and their receptors in the kidneys of these mice. All chemokines and monocyte surface receptors that were decreased in the severely catabolic medulla (figure 6B-G) were also downregulated in whole kidney of this model (figure 6I). *Ccr2* and *Ccr5* decreased significantly in both. Finally, we investigated the

mechanistic role of urea in the murine system in inner medullar collecting duct cells. Indeed, both *Ccl2* and *Ccl5* were upregulated by NaCl and the CCR5 ligand *Ccl5* was significantly decreased by urea (figure 6J). In summary, depression of chemokine expression by urea in vitro reflected decreased chemokine and monocytic marker gene expression in the catabolic kidney medulla in vivo.

NaCl-treated tubular epithelium and its cytokines promote monocyte migration and bacterial killing

Effects of tubular cell stimulation by medullary range NaCl on monocyte migration and function were studied in primary human cells in vitro.

To test for effects of tubular NaCl exposure on monocyte migration, we incubated tubular cells in medullary-range NaCl or equiosmolar urea for 24h and placed monocytes in a transwell above. $CD14^+$ monocytes migrated significantly more towards NaCl-stimulated than control or urea-stimulated epithelium (figure 7A,B, gating in suppl. figure 7A), consistent with induction of chemotactic factors. To delineate effects of the most regulated CCL26 and CCL2, recombinant human cytokines were employed. While CCL2 function is well described [31], less is known about CCL26. Among known human CCL26 receptors [28],[32],[33], expression of CCR1, CCR5 and CX3CR1, but not CCR2 or CCR3 was detected in the normal human medulla (suppl. figure 3B, schematic depiction of putative receptor ligand interactions in C). Both CCL2 and CCL26 increased ERK phosphorylation in human monocytes (figure 7C). In addition, recombinant CCL26 and CCL2 cooperatively enhanced total and $CD14^+$ monocyte migration (figure 7D,E). This is consistent with functional collaboration of these chemokines to induce migration towards NaCl stimulated tubular epithelium. To mimic the medullary situation, chemokine-induced monocyte chemotaxis was assessed in the presence of additional 120mM NaCl. Also here, a combination of CCL2 and CCL26 significantly promoted their migration (figure 7F,G). CCL26 promoted bacterial killing by human blood monocytes (figure 7H,I). In summary, the data demonstrate a cooperative function of CCL2 and CCL26 on monocyte chemotaxis and promotion of bacterial killing.

Tubular CCL26 associates with monocyte distribution in the human kidney

To address a possible role of CCL26 for monocyte distribution in the human kidney, costainings of $CD14^+$ monocytes and $CD68^+$ macrophages with CCL26 were performed in human kidneys (figure 8A). Digitally assisted quantification shows that the proportion of CCL26 expressing tubuli in the renal medulla significantly correlated with medullary $CD14^+$ monocyte densities in both, renal allografts (figure 8B) and native kidneys with minimal change disease (figure 8C). In contrast, there was no association with $CD68^+$ macrophages densities (figure 8D,E) or macrophage polarization markers (suppl. figure 8). Consistently, CCL26 did not affect M1 or M2 marker expression during macrophage differentiation from human monocytes in vitro (suppl. figure 9). More monocytes were observed close to $CCL26^+$ than $CCL26^-$ tubuli in the same kidney (figure 8F). CCL26 correlation with monocyte concentration is consistent with a functional role for their migration in the human kidney.

Discussion

Our data demonstrate that the chief renal osmolytes NaCl and urea exert differential effects on renal tubular epithelial cell chemokine production. They determine CCL26 as a novel NaCl-induced human cytokine with monocyte chemoattractive function.

The knowledge of immunoregulatory roles of osmolarity and tonicity has rapidly advanced in recent years [34],[35]. Compared to other organs, the kidney reaches extreme osmolyte concentrations. In addition, it regulates fluid and electrolyte balance of the whole body. Thus, the local milieu is the result of a complex interplay of systemic and local electrolyte systems. We addressed the roles of the main renal osmolytes, NaCl and urea [1],[2] for tubular cells as a major renal resident celltype producing chemotactic cytokines [11],[18] together with monocytes as major mobile effectors and regulators of renal antibacterial defense [12],[36], and also detrimental inflammation [13].

We found that in tubular epithelium, NaCl enhanced cytokine expression. These NaCl effects were largely substance independent and similarly elicited by elevated tonicity, i.e. by mannitol. This is similar to cytokine regulation in human intestinal and bronchial epithelial and peripheral blood

mononuclear cells [37]–[39]. Chemokine induction required reactive oxygen species, which agrees with mechanisms of hypertonic stimulation in other cell types and settings [20],[22],[40].

Our data introduce CCL26 as a novel monocyte attractant in the human kidney. It was strongly induced by NaCl in vitro and prominent in the human renal medulla, adding renal tubular epithelium to the known CCL26 producers bronchial epithelial cells [24],[25], endothelium [41] and fibroblasts [24],[26]. CCL26, which is a pseudogene in mice [28], was previously detected in human kidney transplants [42]. It was first described as moderate eosinophil chemoattractant and later found to also promote NK cell and monocyte migration [28],[43]. CCL26 functional effects appear to differ depending on the presence of other cytokines and whether recombinant or chemically synthesized protein is used [28],[32],[33]. Our results demonstrate a cooperative function with CCL2 in classical monocyte attraction. Recruited monocytic cells can replace myeloid cells of embryonic origin and develop similar phenotypes in the kidney, as demonstrated in murine models of cell fate mapping [16],[17]. Human renal myeloid cell fates are technically challenging to verify. Our data demonstrating that CCL26 modulates monocytic cell function towards more effective bacterial killing are consistent with a functional role of monocyte derived cells in antibacterial response. Effects on other recruited myeloid cells such as granulocytes as major antibacterial effectors remain to be studied. CCL26's murine functional homologues were similarly regulated in the kidney medulla in vivo and by NaCl and urea in murine renal epithelium in vitro, supporting a common regulatory pattern in these mammalian species. Consistently, monocyte, but not macrophage densities in the human renal medulla correlated with CCL26 protein and gradients were decreased in conditions with a loss of NaCl gradient.

Urea, the other main medullary osmolyte, either did not affect or even dampened tubular chemokine production, namely human *CCL26* and murine *Ccl5*. These effects did not significantly depend on earlier defined mechanisms [44] (data not shown). Their underlying signaling remains to be determined. NaCl intake and hypernatremia cause catabolism in humans and mice [2],[3],[45] and increase renal medullary urea content [2],[3]. As no catabolic patient cohorts who underwent kidney biopsies were identified, we analyzed renal gene expression in two independent datasets of short- and

a long-term catabolic mice. Both show downregulation of chemokine and cognate receptor expression, most markedly with concomitant severe antidiuresis [21],[30]. This is consistent with tubular cell chemokine depression that was elicited by urea in both murine and human cells in vitro.

Systemic NaCl improves immune response to most, but not all infections at sites other than the kidney [3],[46]–[49]. This applies especially to increased local NaCl concentrations, which were however mostly markedly lower than in our study. Our results are consistent with a local proinflammatory function of renal medullary-range NaCl by induction of tubular cell chemokine expression, extending earlier observations [11],[18], and possibly a previously described direct chemotactic effect [50]. By demonstrating that urea is dampening or inert, our data propose novel mechanisms how catabolism decreases renal host defense. This project focused on chemokine regulation by urea and NaCl. Their role in regulation of other immunoregulatory and inflammatory factors including danger signaling and in different inflammatory renal diseases remains to be detailed.

In summary, our results depict two different renal medullary scenarios depending on whether NaCl or urea is the main osmolyte. The energy intense state with tubular cell cytokine production and recruited myeloid cells in the presence of elevated NaCl may aid antibacterial host response. On the other hand, less cytokine production and a stable myeloid cell population in the presence of elevated urea concentrations may benefit an organism with limited energy supply [51]. It may also limit detrimental inflammation. This concept could provide a basis to additional management strategies of these patient populations.

Materials and Methods

Human renal tissue samples

Normal renal tissue was identified in tumor nephrectomy specimens by a licensed renal pathologist (n=8, 13% male, age 61.1 years, range 39-75 years). Renal transplant surveillance biopsies were identified during a previous screening of all adult first renal transplant recipients at Hannover Medical School, conducted according to the declaration of Istanbul, in 2010 for patients who underwent surveillance biopsies. CD68 staining has been reported [19]. In the present study, all transplant biopsy samples with available cortex and medullary tissue were stained for CD14 (n=27).

Clinical chemistry values were assessed in the MHH clinical laboratories. Immunosuppressant and diuretic use and dose (furosemide or torasemide, torasemide dose was multiplied by four to express the biological equivalent) at first outpatient presentation were extracted from the clinical records. For selection of minimal change disease samples, all kidney biopsies performed at MHH in adult patients with an exclusive diagnosis of minimal change disease from 2009-2019 were identified from the archives at the institute for pathology. Clinical data, immunosuppressant and diuretic were extracted from the records. All patients (n=11) with residual cortical and medullary tissue for staining who did not receive immunosuppressants at time of biopsy were included into this study. Immunostaining and microscopy techniques are detailed in the online supplement.

Human and murine cell culture, hyperosmolar stimulation and bacterial killing

HK2 human tubular cells and murine inner medullary collecting duct cells (IMCD, both: ATTC, Manassas, VA). A gene expression profile consistent with proximal tubular cells was ascertained in the gene array. Leukocytes and normal human serum were recovered from fresh blood or anonymized buffy coats obtained as a waste product from the blood donor service. Human peripheral blood mononuclear cells were enriched by density gradient centrifugation with Biocoll 1.077 (Biochrom, Berlin, Germany). Hyperosmolar stimulation, and assessment of monocyte migration, macrophage differentiation and bacterial killing are described in the online supplement.

Quantification of mRNA and soluble protein

RNA isolation, qPCR and ELISA procedures were essentially as described [20] and are detailed in the online supplement together with the primer sequences.

Microarray specification and gene expression dataset analyses

A refined version of the whole human genome oligo microarray 4x44K (V2, ID 026652, Agilent Technologies) called '026652QM_RCUG_HomoSapiens' (ID084555) developed by the Transcriptomics Core was used as described [52]. Data are available as GSE159238. For generation of heatmaps and principal component analysis (PCA) plots, normalized microarray data were imported into OmicsExplorer (V3.3, Qlucore).

Gene array data from normal human kidney (GSE3931)[23] and cortex and inner stripe of

outer medulla of murine control and catabolic kidney (n=3-5 female mice/group, GSE81741)[21] were obtained at NCBI. PANTHER overrepresentation test (V14.1, http://www.pantherdb.org) with Fisher's exact test and Bonferroni correction and the Reactome analysis tool at reactome.org [53] were employed for identification of functional gene groups. Calculation of -log10 adjusted p-values and log-fold changes of candidate genes of the longterm starvation RNA sequencing dataset compared to control mice [30] (n=4 male mice/group) was performed with the public online application of this project.

Flow cytometry

Staining reagents are listed in the online supplement. Flow cytometry analysis was performed on a Becton-Dickinson FACSCanto (Franklin Lakes, NJ) according to the current guidelines [54]. Data were analyzed using FlowJo software (Tree Star Inc., Ashland, OR).

Statistics

Two-tailed student's t-test with Welch's correction if variance was unequal was used to compare two conditions using GraphPadPrism Version 8.2.1 (Irvine, CA). If more than two conditions were compared, Bonferroni's test of selected conditions or Dunnet's test was applied after ANOVA or non-parametric test was employed as appropriate and indicated in the figure legends. Data are expressed as mean±SEM. P-values<0.05 were considered significant and are indicated: *p<0.05, **p<0.01, ***p<0.001.

Data availability statements

All datasets have been uploaded to a public database and will be made publicly available upon publication of the manuscript (GSE159238).

Conflict of interest

The authors declare no commercial or financial conflict of interest

Ethics approval statement

Leukocytes and normal human serum and renal biopsies were analyzed after local ethics board approval (MHH 807, 3516 and 10183).

Author contributions

JS, NB, HH and SvV designed research, JS, NB, AMH, MF conducted experiments, JS, NB, TG, JHB and SvV analyzed data, JS, NB and SvV wrote the manuscript with help from all coauthors, all authors approved the manuscript.

Acknowledgements

We would like to thank all patients for making their samples available to research, T. Tuchel, E. Christians, M. Taleb-Naghsh, J. Jost and the Laser Microscopy and Transcriptomics Core facilities at Hannover Medical School for expert technical assistance. NB was supported by a Hannover Biomedical Research School stipend, JS and JHB by Jackstädt Stiftung and German Ministry for Education and Research (BMBF 13GW0399B), and SvV by grants from MHH HilF2019 and MHH Transplant Centre and Deutsche Forschungsgemeinschaft (450775971 and EXC2151 – 390873048).

References

1. **Sands JM**, **Layton HE**. Advances in Understanding the Urine-Concentrating Mechanism. 2014:26.

2. **Kitada K, Daub S, Zhang Y, Klein JD, Nakano D, Pedchenko T, Lantier L, *et al.*** High salt intake reprioritizes osmolyte and energy metabolism for body fluid conservation. *J Clin Invest*. 2017; **127**:1944–1959.DOI: 10.1172/JCI88532.

3. **Jobin K, Stumpf NE, Schwab S, Eichler M, Neubert P, Rauh M, Adamowski M, *et al.*** A high-salt diet compromises antibacterial neutrophil responses through hormonal perturbation. *Sci. Transl. Med.* 2020; **12**:eaay3850.DOI: 10.1126/scitranslmed.aay3850.

4. **Grist JT, Riemer F, Hansen ESS, Tougaard RS, McLean MA, Kaggie J, Bøgh N, *et al.*** Visualization of sodium dynamics in the kidney by magnetic resonance imaging in a multi-site study. *Kidney International*. 2020; **98**:1174–1178.DOI: 10.1016/j.kint.2020.04.056.

5. **Sheen MR, Kim J-A, Lim SW, Jung J-Y, Han K-H, Jeon US, Park S-H, *et al.*** Interstitial tonicity controls TonEBP expression in the renal medulla. *Kidney International*. 2009; **75**:518–525.DOI: 10.1038/ki.2008.601.

6. **Sone M**, **Albrecht GJ**, **Dorge A**, **Thurau K**, **Beck FX**. Osmotic adaptation of renal medullary cells during transition from chronic diuresis to antidiuresis. *American Journal of Physiology-Renal Physiology*. 1993; **264**:F722–F729.DOI: 10.1152/ajprenal.1993.264.4.F722.

7. **Fernández-Llama P**. Concentrating defect in experimental nephrotic syndrome: Altered expression of aquaporins and thick ascending limb Na+ transporters. :10.

8. **Matar RNB**, **Malik B**, **Wang XH**, **Martin CF**, **Eaton DC**, **Sands JM**, **Klein JD**. Protein abundance of urea transporters and aquaporin 2 change differently in nephrotic pair-fed vs. non-pair-fed rats. *Renal Physiol*.:9.

9. **Ching C**, **Schwartz L**, **Spencer JD**, **Becknell B**. Innate immunity and urinary tract infection. *Pediatr Nephrol*. 2020; **35**:1183–1192.DOI: 10.1007/s00467-019-04269-9.

10. **Abraham SN**, **Miao Y**. The nature of immune responses to urinary tract infections. *Nat Rev Immunol*. 2015; **15**:655–663.DOI: 10.1038/nri3887.

11. **Berry MR, Mathews RJ, Ferdinand JR, Jing C, Loudon KW, Wlodek E, Dennison TW, *et al.*** Renal Sodium Gradient Orchestrates a Dynamic Antibacterial Defense Zone. *Cell*. 2017; **170**:860-874.e19.DOI: 10.1016/j.cell.2017.07.022.

12. **Schiwon M, Weisheit C, Franken L, Gutweiler S, Dixit A, Meyer-Schwesinger C, Pohl J-M, *et al.*** Crosstalk between Sentinel and Helper Macrophages Permits Neutrophil Migration into Infected Uroepithelium. *Cell*. 2014; **156**:456–468.DOI: 10.1016/j.cell.2014.01.006.

13. **Tang PM-K**, **Nikolic-Paterson DJ**, **Lan H-Y**. Macrophages: versatile players in renal inflammation and fibrosis. *Nat Rev Nephrol*. 2019; **15**:144–158.DOI: 10.1038/s41581-019-0110-2.

14. **Stewart BJ, Ferdinand JR, Young MD, Mitchell TJ, Loudon KW, Riding AM, Richoz N, *et al.*** Spatiotemporal immune zonation of the human kidney. *Science*. 2019; **365**:1461–1466.DOI: 10.1126/science.aat5031.

15. **Hoeffel G, Chen J, Lavin Y, Low D, Almeida FF, See P, Beaudin AE, *et al.*** C-Myb(+) erythro-myeloid progenitor-derived fetal monocytes give rise to adult tissue-resident macrophages. *Immunity*. 2015; **42**:665–678.DOI: 10.1016/j.immuni.2015.03.011.

16. **Ide S, Yahara Y, Kobayashi Y, Strausser SA, Ide K, Watwe A, Xu-Vanpala S, *et al.*** Yolk-sac-derived macrophages progressively expand in the mouse kidney with age. *Elife*. 2020; **9**:e51756.DOI: 10.7554/eLife.51756.

17. **Liu F, Dai S, Feng D, Qin Z, Peng X, Sakamuri SSVP, Ren M, *et al.*** Distinct fate, dynamics and niches of renal macrophages of bone marrow or embryonic origins. *Nat Commun*. 2020; **11**:2280.DOI: 10.1038/s41467-020-16158-z.

18. **Casper J, Schmitz J, Bräsen JH, Khalifa A, Schmidt BMW, Einecke G, Haller H, *et al.*** Renal transplant recipients receiving loop diuretic therapy have increased urinary tract infection rate and altered medullary macrophage polarization marker expression. *Kidney International*. 2018; **94**:993–1001.DOI: 10.1016/j.kint.2018.06.029.

19. **Bräsen JH, Khalifa A, Schmitz J, Dai W, Einecke G, Schwarz A, Hallensleben M, *et al.*** Macrophage density in early surveillance biopsies predicts future renal transplant function. *Kidney International*. 2017; **92**:479–489.DOI: 10.1016/j.kint.2017.01.029.

20. **Helmke A, Hüsing AM, Gaedcke S, Brauns N, Balzer MS, Reinhardt M, Hiss M, *et al.*** Peritoneal dialysate- range hypertonic glucose promotes T- cell IL- 17 production that induces mesothelial inflammation. *Eur. J. Immunol.* 2020:eji.202048733.DOI: 10.1002/eji.202048733.

21. **Xu K, Rosenstiel P, Paragas N, Hinze C, Gao X, Huai Shen T, Werth M, *et al.*** Unique Transcriptional Programs Identify Subtypes of AKI. *JASN*. 2017; **28**:1729–1740.DOI: 10.1681/ASN.2016090974.

22. **Zhou X**, **Ferraris JD**, **Cai Q**, **Agarwal A**, **Burg MB**. Increased reactive oxygen species contribute to high NaCl-induced activation of the osmoregulatory transcription factor TonEBP/OREBP. *American Journal of Physiology-Renal Physiology*. 2005; **289**:F377–F385.DOI: 10.1152/ajprenal.00463.2004.

23. **Higgins JPT, Wang L, Kambham N, Montgomery K, Mason V, Vogelmann SU, Lemley KV, *et al.*** Gene Expression in the Normal Adult Human Kidney Assessed by Complementary DNA Microarray. *MBoC*. 2004; **15**:649–656.DOI: 10.1091/mbc.e03-06-0432.

24. **Banwell ME**, **Tolley NS**, **Williams TJ**, **Mitchell TJ**. REGULATION OF HUMAN EOTAXIN-3/CCL26 EXPRESSION: MODULATION BY CYTOKINES AND GLUCOCORTICOIDS. *Cytokine*. 2002; **17**:317–323.DOI: 10.1006/cyto.2002.1021.

25. **Coleman S**, **Kruger M**, **Sawyer G**, **Hurst R**. Procyanidin A2 Modulates IL-4-Induced CCL26 Production in Human Alveolar Epithelial Cells. *IJMS*. 2016; **17**:1888.DOI: 10.3390/ijms17111888.

26. **Hebenstreit D**, **Luft P**, **Schmiedlechner A**, **Duschl A**, **Horejshoeck J**. SOCS-1 and SOCS-3 inhibit IL-4 and IL-13 induced activation of Eotaxin-3/CCL26 gene expression in HEK293 cells. *Molecular Immunology*. 2005; **42**:295–303.DOI: 10.1016/j.molimm.2004.09.004.

27. **Larose M-C**, **Chakir J**, **Archambault A-S**, **Joubert P**, **Provost V**, **Laviolette M**, **Flamand N**. Correlation between CCL26 production by human bronchial epithelial cells and airway eosinophils: Involvement in patients with severe eosinophilic asthma. *Journal of Allergy and Clinical Immunology*. 2015; **136**:904–913.DOI: 10.1016/j.jaci.2015.02.039.

28. **Nakayama T, Watanabe Y, Oiso N, Higuchi T, Shigeta A, Mizuguchi N, Katou F, *et al.*** Eotaxin-3/CC Chemokine Ligand 26 Is a Functional Ligand for CX3CR. *The Journal of Immunology*.:9.

29. **Takao K**, **Miyakawa T**. Genomic responses in mouse models greatly mimic human inflammatory diseases. *Proc Natl Acad Sci U S A*. 2015; **112**:1167–1172.DOI: 10.1073/pnas.1401965111.

30. **Johnsen M, Kubacki T, Yeroslaviz A, Späth MR, Mörsdorf J, Göbel H, Bohl K, *et al.*** The Integrated RNA Landscape of Renal Preconditioning against Ischemia-Reperfusion Injury. *JASN*. 2020; **31**:716–730.DOI: 10.1681/ASN.2019050534.

31. **Shi C**, **Pamer EG**. Monocyte recruitment during infection and inflammation. *Nat Rev Immunol*. 2011; **11**:762–774.DOI: 10.1038/nri3070.

32. **Ogilvie P**, **Paoletti S**, **Clark-Lewis I**, **Uguccioni M**. Eotaxin-3 is a natural antagonist for CCR2 and exerts a repulsive effect on human monocytes. *Blood*. 2003; **102**:789–794.DOI: 10.1182/blood-2002-09-2773.

33. **Petkovic V**, **Moghini C**, **Paoletti S**, **Uguccioni M**, **Gerber B**. A HUMAN CHEMOKINE WITH A REGULATORY ROLE. :8.

34. **Müller DN**, **Wilck N**, **Haase S**, **Kleinewietfeld M**, **Linker RA**. Sodium in the microenvironment regulates immune responses and tissue homeostasis. *Nat Rev Immunol*. 2019; **19**:243–254.DOI: 10.1038/s41577-018-0113-4.

35. **Aramburu J**, **López-Rodríguez C**. Regulation of Inflammatory Functions of Macrophages and T Lymphocytes by NFAT5. *Front Immunol*. 2019; **10**:535.DOI: 10.3389/fimmu.2019.00535.

36. **Engel DR, Maurer J, Tittel AP, Weisheit C, Cavlar T, Schumak B, Limmer A, *et al.*** CCR2 mediates homeostatic and inflammatory release of Gr1(high) monocytes from the bone marrow, but is dispensable for bladder infiltration in bacterial urinary tract infection. *J Immunol*. 2008; **181**:5579–5586.DOI: 10.4049/jimmunol.181.8.5579.

37. **Hashimoto S**, **Matsumoto K**, **Gon Y**, **Nakayama T**, **Takeshita I**, **Horie T**. Hyperosmolarity-induced Interleukin-8 Expression in Human Bronchial Epithelial Cells through p38 Mitogen-activated Protein Kinase. *Am J Respir Crit Care Med*. 1999; **159**:634–640.DOI: 10.1164/ajrccm.159.2.9712090.

38. **Shapiro L**, **Dinarello CA**. Osmotic regulation of cytokine synthesis in vitro. *Proceedings of the National Academy of Sciences*. 1995; **92**:12230–12234.DOI: 10.1073/pnas.92.26.12230.

39. **Németh ZH**, **Deitch EA**, **Szabó C**, **Haskó G**. Hyperosmotic Stress Induces Nuclear Factor-κB Activation and Interleukin-8 Production in Human Intestinal Epithelial Cells. *The American Journal of Pathology*. 2002; **161**:987–996.DOI: 10.1016/S0002-9440(10)64259-9.

40. **Ip WKE**, **Medzhitov R**. Macrophages monitor tissue osmolarity and induce inflammatory response through NLRP3 and NLRC4 inflammasome activation. *Nat Commun*. 2015; **6**:6931.DOI: 10.1038/ncomms7931.

41. **Shinkai A, Yoshisue H, Koike M, Shoji E, Nakagawa S, Saito A, Takeda T, *et al.*** A novel human CC chemokine, eotaxin-3, which is expressed in IL-4-stimulated vascular endothelial cells, exhibits potent activity toward eosinophils. *J Immunol*. 1999; **163**:1602–1610.

42. **Wohlfahrtova M**, **Tycova I**, **Honsova E**, **Lodererova A**, **Viklicky O**. Molecular patterns of subclinical and clinical rejection of kidney allograft: quantity matters. *Kidney Blood Press Res*. 2015; **40**:244–257.DOI: 10.1159/000368500.

43. **El-Shazly AE**, **Doloriert HC**, **Bisig B**, **Lefebvre PP**, **Delvenne P**, **Jacobs N**. Novel cooperation between CX3CL1 and CCL26 inducing NK cell chemotaxis via CX3CR1: a possible mechanism for NK cell infiltration of the allergic nasal tissue. *Clin Exp Allergy*. 2013; **43**:322–331.DOI: 10.1111/cea.12022.

44. **Tian W**, **Cohen DM**. Urea stress is more akin to EGF exposure than to hypertonic stress in renal medullary cells. *Am J Physiol Renal Physiol*. 2002; **283**:F388-398.DOI: 10.1152/ajprenal.00031.2002.

45. **McLaughlan E**, **Barth JH**. An analysis of the relationship between serum cortisol and serum sodium in routine clinical patients. *Practical Laboratory Medicine*. 2017; **8**:30–33.DOI: 10.1016/j.plabm.2017.04.003.

46. **Sailer CO**, **Wiedemann SJ**, **Strauss K**, **Schnyder I**, **Fenske WK**, **Christ-Crain M**. Markers of systemic inflammation in response to osmotic stimulus in healthy volunteers. *Endocr Connect*. 2019; **8**:1282–1287.DOI: 10.1530/EC-19-0280.

47. **Jantsch J, Schatz V, Friedrich D, Schröder A, Kopp C, Siegert I, Maronna A, *et al.*** Cutaneous Na+ storage strengthens the antimicrobial barrier function of the skin and boosts macrophage-driven host defense. *Cell Metab*. 2015; **21**:493–501.DOI: 10.1016/j.cmet.2015.02.003.

48. **Wenstedt EFE, Verberk SGS, Kroon J, Neele AE, Baardman J, Claessen N, Pasaoglu ÖT, *et al.*** Salt increases monocyte CCR2 expression and inflammatory responses in humans. *JCI Insight*. 2019; **4**:e130508.DOI: 10.1172/jci.insight.130508.

49. **Wilck N, Matus MG, Kearney SM, Olesen SW, Forslund K, Bartolomaeus H, Haase S, *et al.*** Salt-responsive gut commensal modulates TH17 axis and disease. *Nature*. 2017; **551**:585–589.DOI: 10.1038/nature24628.

50. **Müller S, Quast T, Schröder A, Hucke S, Klotz L, Jantsch J, Gerzer R, *et al.*** Salt-Dependent Chemotaxis of Macrophages Ko BCB, ed. *PLoS ONE*. 2013; **8**:e73439.DOI: 10.1371/journal.pone.0073439.

51. **Minegishi S**, **Luft FC**, **Titze J**, **Kitada K**. Sodium Handling and Interaction in Numerous Organs. *American Journal of Hypertension*. 2020; **33**:687–694.DOI: 10.1093/ajh/hpaa049.

52. **Roy-Chowdhury E, Brauns N, Helmke A, Nordlohne J, Bräsen JH, Schmitz J, Volkmann J, *et al.*** Human CD16+ monocytes promote a pro-atherosclerotic endothelial cell phenotype via CX3CR1–CX3CL1 interaction. *Cardiovascular Research*. 2020:cvaa234.DOI: 10.1093/cvr/cvaa234.

53. **Jassal B, Matthews L, Viteri G, Gong C, Lorente P, Fabregat A, Sidiropoulos K, *et al.*** The reactome pathway knowledgebase. *Nucleic Acids Res*. 2020; **48**:D498–D503.DOI: 10.1093/nar/gkz1031.

54. Cossarizza, A., Chang, H. D., Radbruch, A., , Abrignani, S., Addo, R., Akdis, M., Andrä, I., et al., Guidelines for the use of flow cytometry and cell sorting in immunological studies (third edition) Eur. J. Immunol. 2021. 51: 2708–3145

Figure 1: Monocyte distribution in the human renal cortex and medulla and its modulation by loop diuretic therapy

(A-C) $CD68^+$ macrophages and $CD14^+$ monocytes were evaluated in histologically normal human kidney sections. Their abundance as % of all tissue was evaluated in cortex and medulla separately (A, examples, B, statistical evaluation of n=8 patients each evaluated once, paired t-tests, bars indicate 100μm). **(C)** The medullary-cortical gradients of $CD68^+$ macrophage and $CD14^+$ monocyte densities were compared in each individual kidney (n=8 patients, each evaluated once, paired t-test). **(D,E)** $CD14^+$ monocyte medullary-cortical density gradients in human kidney allografts were compared in early surveillance biopsies of patients with and without loop diuretic therapy (D examples, bars indicate 100μm, E n=12 and 15 patients per group, each evaluated once, t-test with Welch's correction). **(F,G)** $CD14^+$ monocyte and $CD68^+$ macrophage medullary-cortical density gradients in human primary minimal change disease specimens were compared in patients without (n=7 patients, each evaluated once) and with loop diuretic therapy at time of biopsy (n=4 patients, each evaluated once) (E: paired t-tests, F examples, bars indicate 100μm). Data are expressed as mean±SEM.

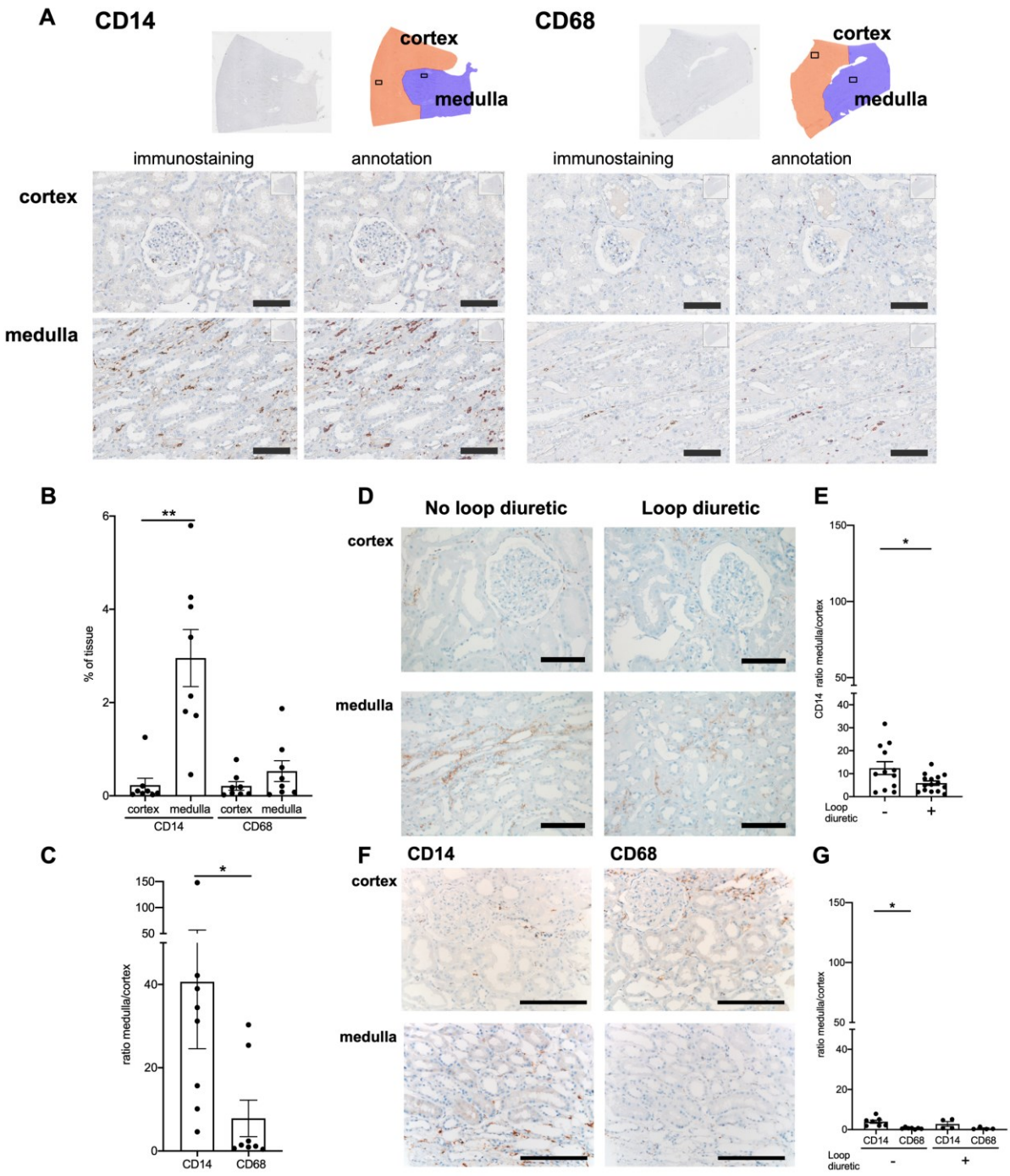

Figure 2: The effect of NaCl and urea on tubular epithelial cell gene expression

(A-D) Human renal tubular epithelial cells (HK2) were exposed to additional 120mM NaCl, isoosmolar Urea (240mM) or mannitol (240mM) as tonicity control. Gene expression was assessed by gene array analysis after 24h (n=1 per condition in one experiment). **(A)** Venn's diagrams of genes regulated twofold or more in parallel are shown for all, up- and downregulated genes of the three hyperosmolar conditions compared to normal media. The proportion of genes regulated by NaCl and urea in the up- and downregulated groups was compared by Fisher's exact test. **(B,C)** Principal component analysis of all regulated genes (B) and with the variance threshold = 0.4 (C). **(D)** Heat map analysis, variance threshold = 0.4.

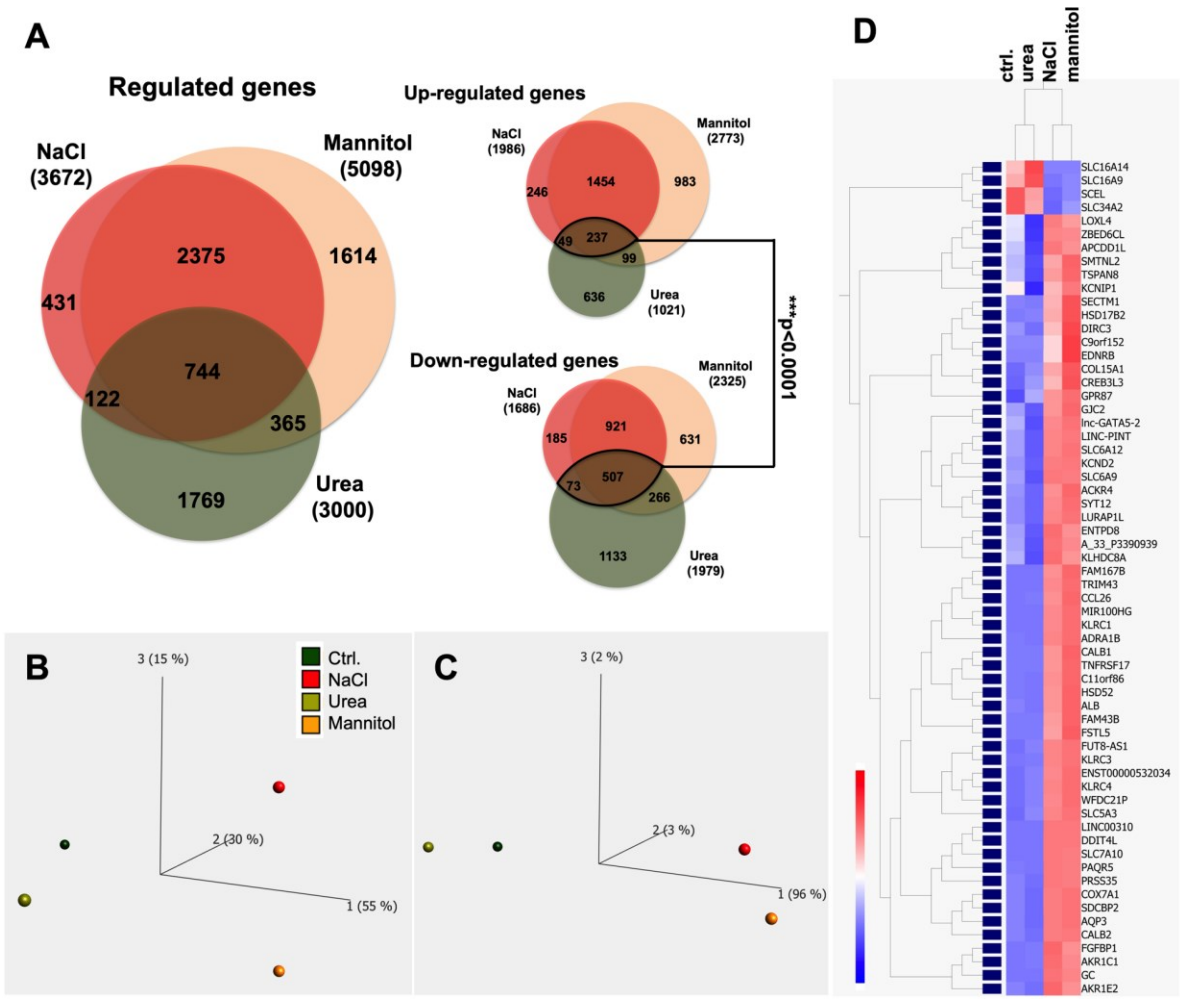

Figure 3: Renal epithelial cell chemotactic cytokine expression response to elevated NaCl and urea

(A-E) Human renal tubular epithelial cells (HK2) were cultured with additional 120mM NaCl, isoosmolar Urea (240mM) or mannitol as tonicity control. **(A,B)** Regulation of soluble immune mediators (chemokines, interleukins, and colony stimulating factors) was assessed by gene array analysis after 24h (experimental conditions as in fig. 2) and is shown relative to control (A, log values). All mediators regulated 1.5x or more are underlaid in gray. **(B)** Volcano plot analysis of iso- versus hypertonic osmolytes shows most upregulation in hypertonicity for CCL26 and CCL2, followed by CSF1. **(C)** Response of the three most regulated mediators CCL26, CCL2 and CSF1 was assessed after 6, 24 and 48h exposure to additional high (+120mM) and low (+40mM) NaCl concentrations and equiosmolar urea by qPCR (n=3 in 3 indep. exp., Dunnett's after ANOVA at each timepoint). **(D)** HK2 were exposed to mannitol as tonicity control, NaCl or urea of equal osmolarity. CCL26, CCL2 and CSF1 mRNA was determined by qPCR (n=3 in 3 indep. exp., Dunnett's after ANOVA). **(E)** ROS-scavenger NAC (10mM) was added to 24h stimulation with the indicated osmolyte concentrations (120mM NaCl, 240mM urea, 60mM NaCl+120mM urea) and chemokine mRNA assessed (n=3 in 3 indep. exp., Sidak's test after ANOVA). Data are expressed as mean±SEM.

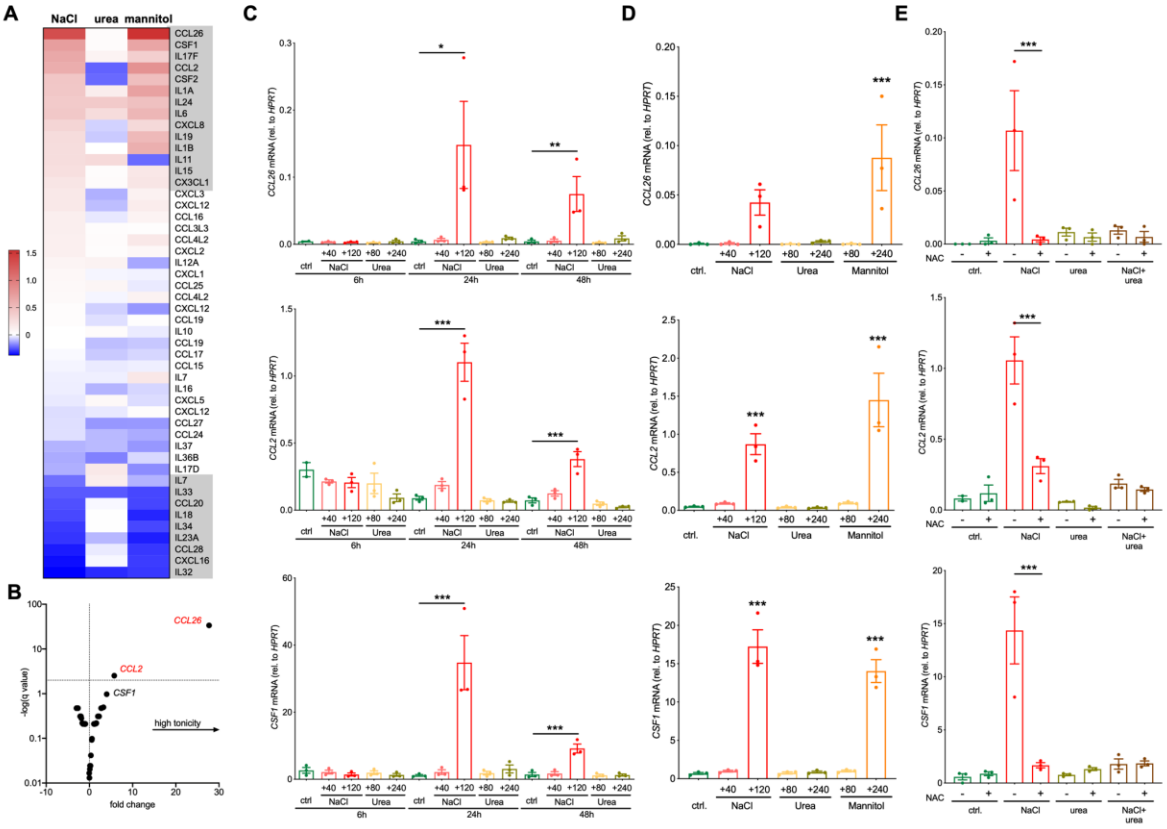

Figure 4: Renal chemotactic cytokine expression in cortex and medulla

(A,B) CCL26 protein (A) and mRNA (B) was assessed in normal tissues from tumor nephrectomies (n=8 patients, each investigated once). **(C)** All chemotactic factors upregulated at least 1.5x by NaCl in tubular epithelium were analyzed in a human kidney outer cortex and inner medulla gene expression set (GSE3931). All genes reported by the array and their individual p-values are shown (n=5 kidneys from 5 patients, each investigated once), log values relative to mean of cortex, whiskers represent total range, p-values of individual t-tests are shown if below 0.2). **(D)** CLL26 expression (red) in relation to proximal tubular markers CD10 and CD138, loop of Henle (LOH) and distal tubular marker EMA, marker of ascending loop of Henle (LOH) cytokeratin (CK)7, and collecting duct marker cytokeratin (CK) 34βE12 (green, blue: DAPI nuclear counterstain, examples of at least 10 HPF per marker, bars=50μm) **(E,F)** The proportion of $CCL26^{+}$ tubuli in cortex and medulla of normal human kidney was assessed after immunostaining on digitalized images using an interactively set threshold based on diaminobenzidine optical density (E examples of staining and tubular annotation, n=8 patients, each tested once, Wilcoxon matched-pairs test, bar=50μm).

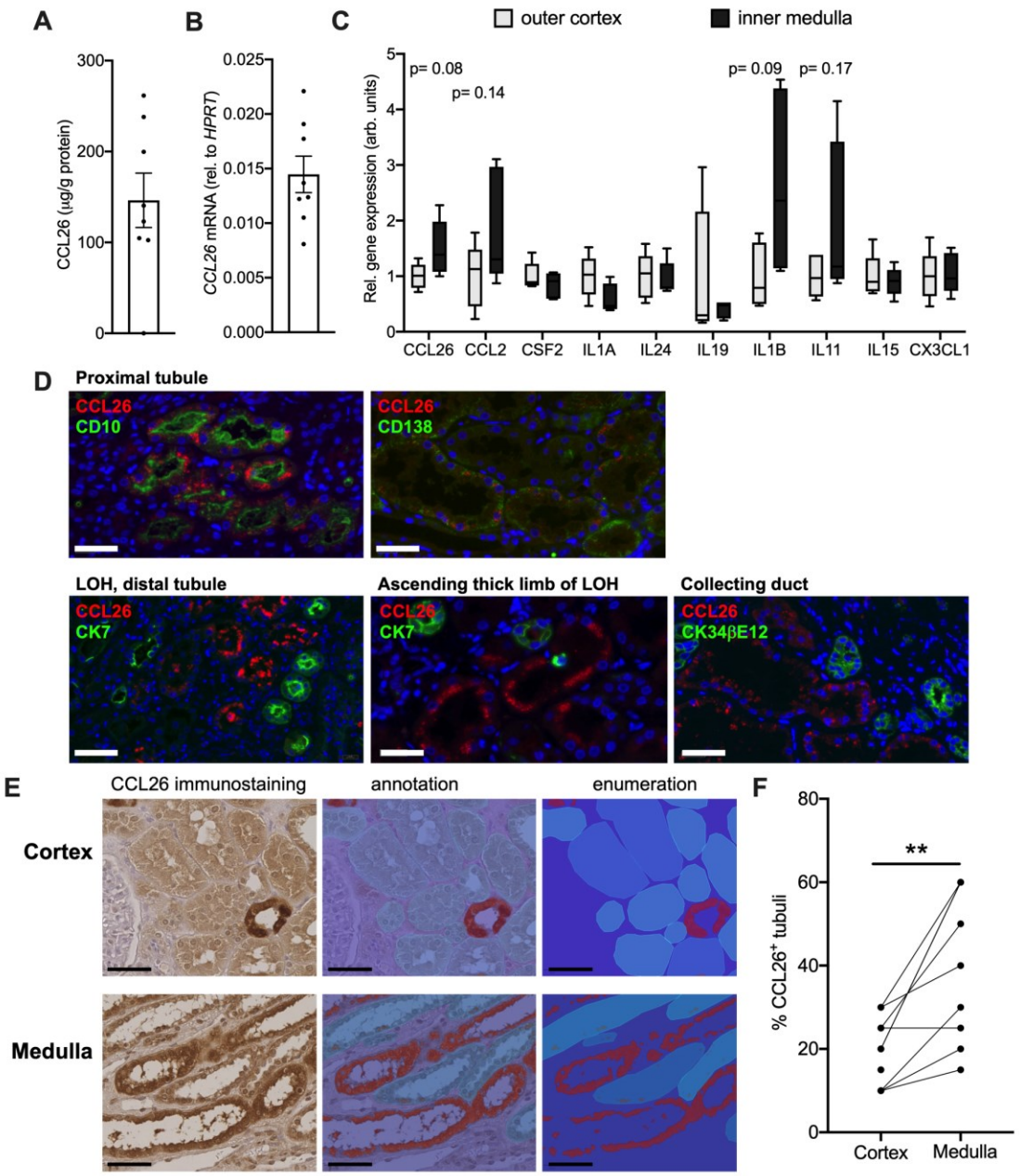

Figure 5: Regulation of monocyte chemotactic factors by urea

(A,B) Human tubular epithelial cells (HK2) were cultured with additional 120mM NaCl, isoosmolar Urea (240mM) or combinations with equal total osmolarity (60mM NaCl + 120mM urea) or substance concentration (120mM NaCl + 240mM urea) (A) or 240mM additional urea in the presence or absence of recombinant IL-4 and IL-13 (1 and 10ng/ml, B) for 24h. *CCL26*, *CCL2* and *CSF1* gene expression was assessed by qPCR (A: n=4 in 4 indep. exp., Dunnett's after ANOVA, B: n=3 in 3 indep. exp., t-tests). Data are expressed as mean±SEM.

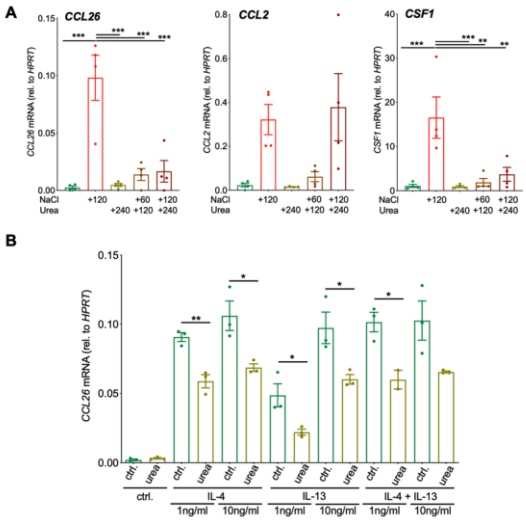

Figure 6: Regulation of monocyte chemotactic factors in the catabolic kidney medulla

(A-G) Gene expression in renal cortex and inner stripe of outer medulla was analyzed in catabolic (cat.) mice after 72h water deprivation and untreated controls (experimental setup in A, GSE81741). Macrophage marker CD68 and murine monocyte marker CD115 (*Csfr1*) (B), monocyte subtype markers and chemokine receptors CCR2 and CX3CR1 (C), M1 and M2 macrophage markers MHCII (*H2Aa*) and CD206 (*Mrc2*) (D) and cognate ligands (E) were assessed (n=3 ctrl., n=5 catabolic mice in one exp., Bonferroni after ANOVA). **(F)** Overview of murine chemokines and their receptors. Genes regulated in human tubular epithelium by NaCl and urea are marked in blue if detected in the murine kidney and red if upregulated in normal medulla compared to cortex *and* downregulated in the medulla in catabolism. Known interactions are marked by arrows. CCL26 is a pseudogene in mice. **(G)** Regulation of CCR5, which is among human CCL26 receptors, and its murine ligands CCL3, CCL4 and CCL5 mRNA expression in murine cortex and medulla at rest and in catabolism. **(H,I)** Total kidney gene expression after four weeks caloric restriction of 70% of normal food intake (H). Relative change and adjusted p-values of all genes analyzed in B-G are shown (I, chemokines in blue, receptors and surface markers in black, significant p-values are indicated above dotted line on y-axis. *Ccl2, Ccl3, Ccl4* and *Ccl5* were below detection limits, n=4/group in one exp.). **(J)** Murine inner medullary collecting duct (IMCD) cells were exposed to the indicated additional NaCl and urea concentrations and *Ccl2* and *Ccl5* chemokine gene expression assessed after 24h. *Ccl3* and *Ccl4* were below detection limit (n=6 from 3 indep. exp., Dunnett's after ANOVA). Data are expressed as mean±SEM.

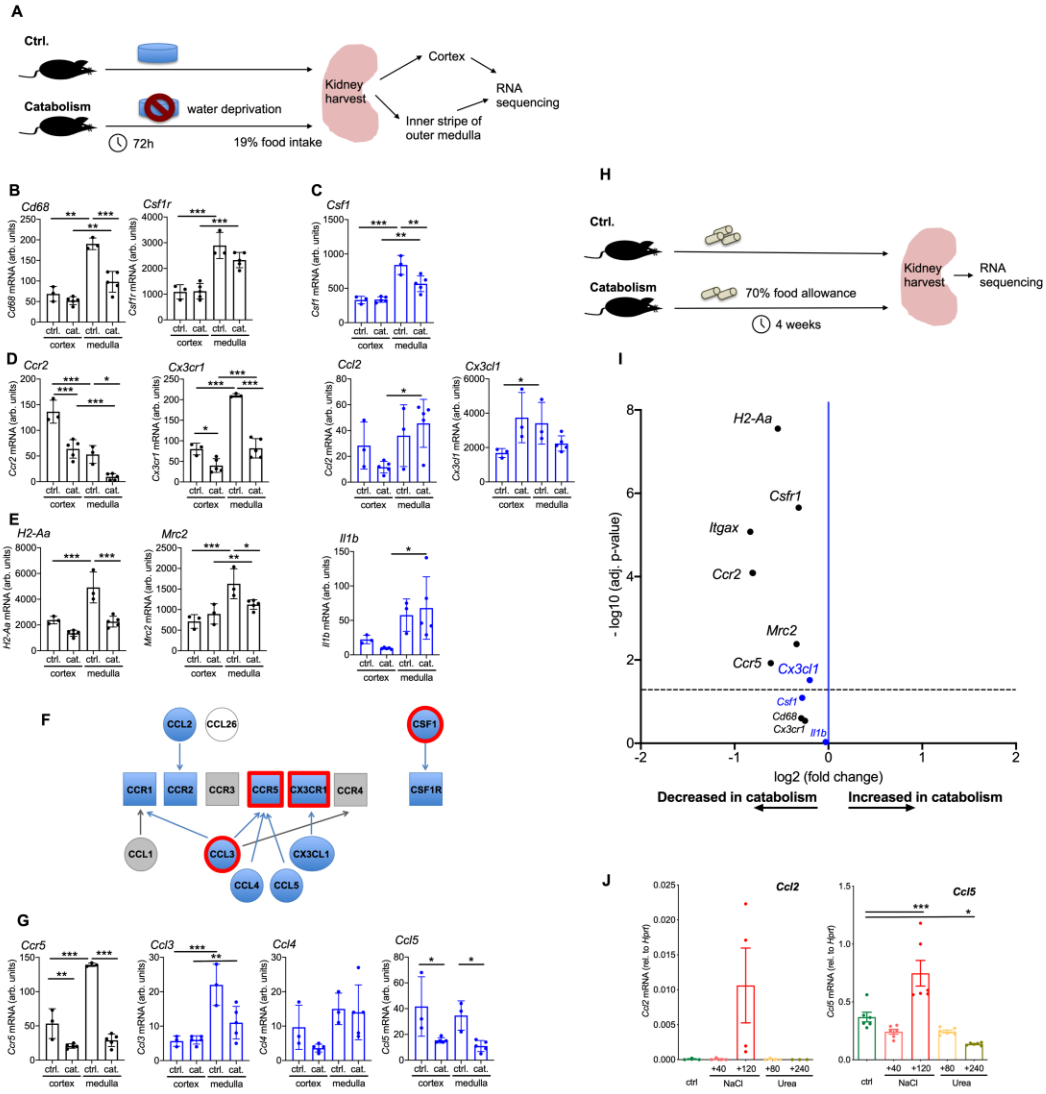

Figure 7: Monocyte migration, differentiation and bacterial killing in response to NaCl-stimulated epithelium and induced chemokines

(A,B) Human renal tubular epithelial cells (HK2) were exposed to additional 120mM NaCl, equiosmolar urea or standard media for 24h. Cells were washed and culture was continued in standard media for 3h. During the last hour, human peripheral blood mononuclear cells were added in a transwell chamber. Monocyte migration was assessed by flow cytometry (experimental setup in A, B: statistical analysis of n=4 from 2 indep. exp., Dunnett's after ANOVA, gating in suppl. figure 7A). **(C)** ERK phosphorylation was assessed in human peripheral blood $CD11b^+$ mononuclear cells after 5min exposure to recombinant CCL2 (10ng/ml) or CCL26 (1000ng/ml) (1 of 2 indep. exp., gating in suppl. figure 7B). **(D,E)** Migration of monocytes in a transwell towards recombinant CCL2 (1ng/ml) or CCL26 (500ng/ml) was assessed by flow cytometry (experimental setup in D, E: statistical analysis of n=4 from 2 separate exp., Dunnett's after ANOVA). **(F,G)** Migration of monocytes in a transwell in media supplemented with 120mM NaCl towards recombinant CCL2 (1ng/ml) or CCL26 (500ng/ml) was assessed after 1h by flow cytometry (experimental setup in F, G: n=4 from 2 separate exp., ratio paired t-tests). **(H,I)** Killing of E. coli during 1h co-incubation with CCL26-prestimulated compared to control monocytes (experimental setup in H, I: n=9 from 9 separate exp., paired t-tests). Data are expressed as mean±SEM.

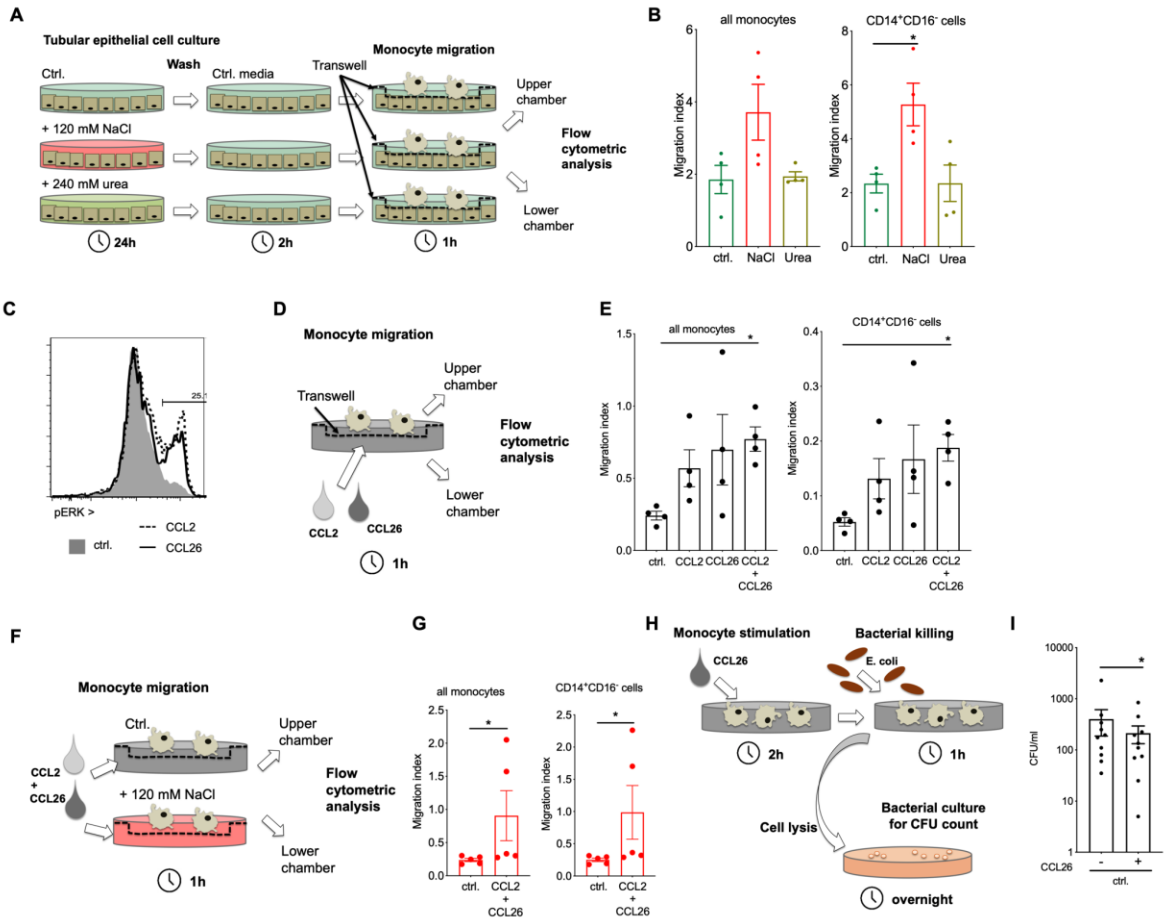

Figure 8: Correlation of CCL26 and monocyte abundance in the human renal medulla

(A-E) $CD14^+$ monocyte (B,C) and $CD68^+$ macrophage (D,E) densities in renal medulla of renal transplant recipients (B,D) and patients with minimal change disease (C,E) are shown in relation to tubular CCL26 expression (A, examples of cortex in medulla with high and low CCL26 densities, cohorts as in figure 1 and suppl. tables 1,2). **(F)** The number of $CD14^+$ monocytes within 10µm of $CCL26^+$ versus $CCL26^-$ tubules was compared (n=15 tubuli from 1 patient evaluated once, Mann-Whitney test. Data are expressed as mean±SEM.

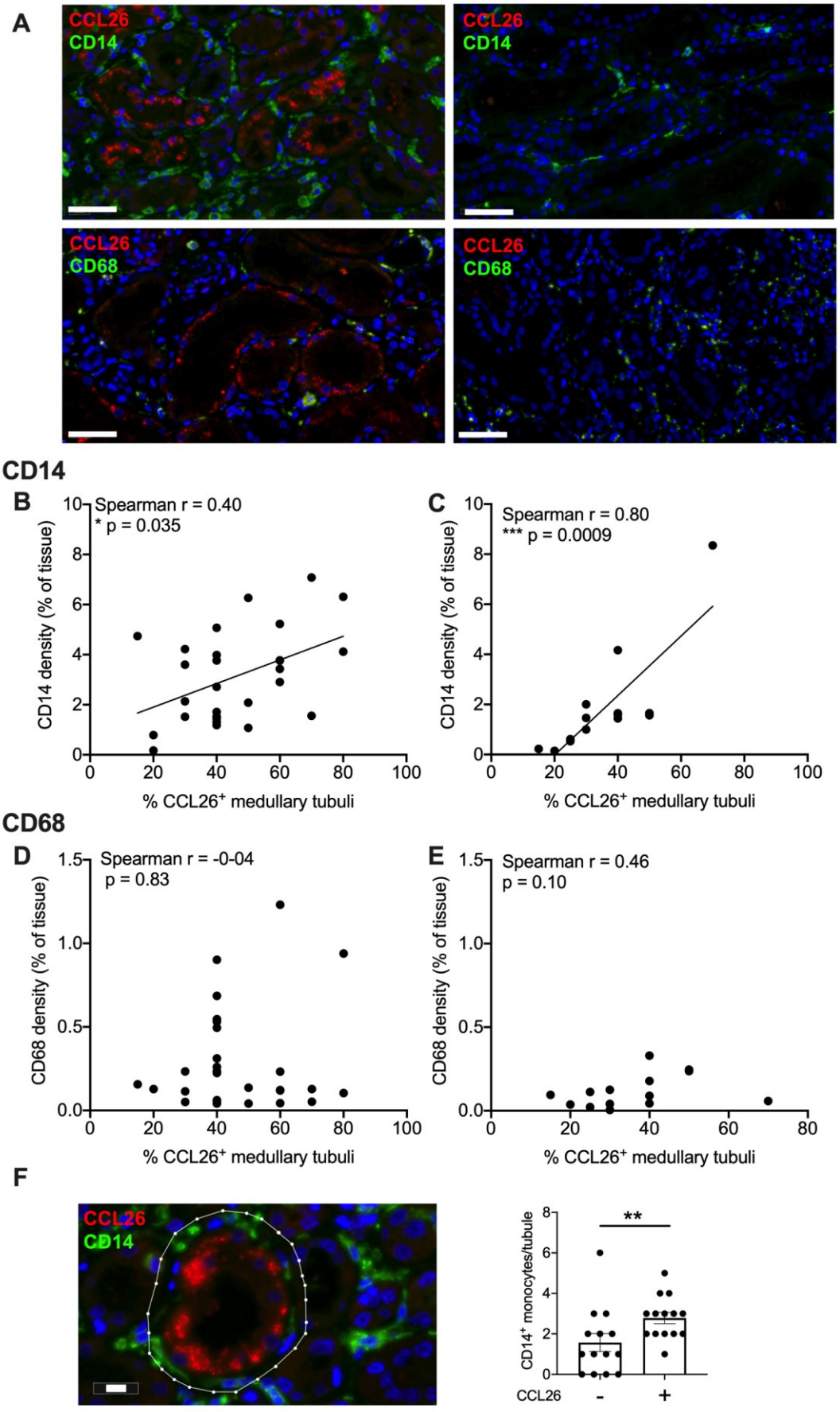

Graph Abstract

Immune cells in the kidney serve as sentinels against ascending bacteria but also promote detrimental inflammation. The kidney medulla is characterized by extreme electrolyte concentrations. We here show that renal medullary range NaCl induces tubular cell chemokine expression and delineate human CCL26 as a novel monocyte chemotactic factor.